



OPEN

Ultrafast intersystem-crossing in platinum containing π -conjugated polymers with tunable spin-orbit couplingC.-X. Sheng^{1,2*}, S. Singh^{1*}, A. Gambetta^{1*†}, T. Drori¹, M. Tong¹, S. Tretiak³ & Z. V. Vardeny¹

SUBJECT AREAS:

ORGANIC LEDs
NONLINEAR OPTICS
CHEMICAL PHYSICS
MOLECULAR ELECTRONICSReceived
24 April 2013Accepted
22 August 2013Published
13 September 2013Correspondence and
requests for materials
should be addressed to
Z.V.V. (val@physics.
utah.edu)* These authors
contributed equally to
this work.† Current address:
Dipartimento di Fisica,
Politecnico di Milano,
Piazza L. da Vinci 32, I-
20133 Milano, Italy.¹Department of Physics & Astronomy, University of Utah, Salt Lake City, Utah 84112, USA, ²School of Electronic and Optical Engineering, Nanjing University of Science and Technology, Nanjing, Jiangsu, 210094, China, ³Theoretical Division, Center for Nonlinear Studies (CNLS), and Center for Integrated Nanotechnologies (CINT), Los Alamos National Laboratory, Los Alamos, New Mexico 87545, USA.

The development of efficient organic light-emitting diodes (OLED) and organic photovoltaic cells requires control over the dynamics of spin sensitive excitations. Embedding heavy metal atoms in π -conjugated polymer chains enhances the spin-orbit coupling (SOC), and thus facilitates intersystem crossing (ISC) from the singlet to triplet manifolds. Here we use various nonlinear optical spectroscopies such as two-photon absorption and electroabsorption in conjunction with electronic structure calculations, for studying the energies, emission bands and ultrafast dynamics of spin photoexcitations in two newly synthesized π -conjugated polymers that contain intrachain platinum (Pt) atoms separated by one (Pt-1) or three (Pt-3) organic spacer units. The controllable SOC in these polymers leads to a record ISC time of $< \sim 1$ ps in Pt-1 and ~ 6 ps in Pt-3. The tunable ultrafast ISC rate modulates the intensity ratio of the phosphorescence and fluorescence emission bands, with potential applications for white OLEDs.

The dynamics of spin singlet and triplet excitations in π -conjugated polymers define their performance as active layer in OLEDs and organic photovoltaic (OPV) cells. For example, if both triplet and singlet excitons can be used in OLEDs to convert electrical energy to electroluminescence emission, then the fraction of excitons that potentially can emit light may reach 100%^{1,2}. Similarly in OPV based on donor/acceptor (D-A) blends, the photogenerated singlet exciton in the polymer donor domains may recombine before reaching the D-A interface, because of its relatively short life time (~ 100 ps). In contrast, because of the much longer life time (~ 5 μ s), triplet excitons could be the answer to this loss mechanism^{3,4}. Therefore, both OLED and OPV technologies may substantially benefit from the proper use of the spin triplet states. Alas, because the SOC in polymers is typically very weak, triplet excitons cannot be efficiently photogenerated in the donor polymers for OPV enhancement; and, similarly, cannot efficiently emit light in OLEDs. The SOC however can be enhanced by embedding heavy atoms such as platinum (Pt) in the polymer backbone chains. Such enhanced SOC, in turn may increase the ISC rate from the singlet-to-triplet manifold, which would make triplet excitons more viable for OPV applications. In addition, the enhanced SOC may also trigger substantive phosphorescence (PH) emission from the lowest triplet state^{5,6}, and thus the emission spectrum from such semiconductor polymers may contain both fluorescence (FL) and PH bands. In fact, these two bands span the visible spectral range, and therefore may potentially be used in designing 'white' electroluminescence emission from the same polymer in OLEDs, with internal quantum efficiency approaching 100%⁷.

These beneficial triplet characteristic properties are the main reason that a variety of Pt-containing polymers have been synthesized and studied. Most of these studies however have been focused on the photophysics of the triplet excitons^{8,9}. Importantly, the dynamics of the internal conversion and ISC processes have not been elucidated, and a complete description of the essential electronic excited states involved is still lacking. For example, the metal-to-ligand charge-transfer (MLCT) state, which has been studied extensively in metal-organic complexes^{10,11}, has not been properly addressed in Pt-containing polymers. In the present work we use a broad arsenal of linear and nonlinear optical (NLO) spectroscopies, complemented with electronic structure calculations, for studying the photoexcitations dynamics in two Pt-containing π -conjugated polymers with different π -conjugated spacer unit length between the nearest Pt atoms on the chain, which controls the spin dynamics of excited states, namely the timescales of the ISC process in this class of materials.

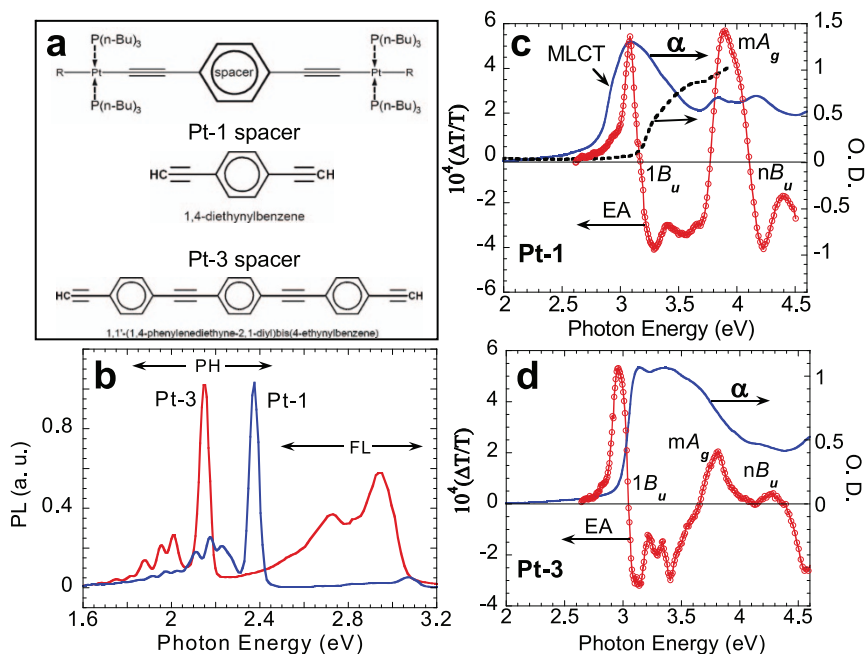


Figure 1 | Linear and NLO measurements of the Pt-polymers. (a), Chemical structures of the two Pt-polymers, where the “spacer” in Pt-1 has a single phenyl ring, whereas that of Pt-3 has three phenyl rings. (b), Normalized photoluminescence emission spectrum of Pt-1 (blue) and Pt-3 (red) films. FL (PH) stands for fluorescence (phosphorescence) emission. (c) and (d), Electroabsorption (EA) spectra of Pt-1 (c) and Pt-3 (d) films, compared to their respective absorption (α) spectrum. The absorption of a non-Pt polymer film is also shown (broken line) in (c). The three excited “essential states” $1B_u$, mA_g , and nB_u , as well as the novel state, Metal-to-Ligand Charge Transfer (MLCT) are assigned.

The backbone structures of the two Pt-polymers that we studied are shown in Figure 1(a); the *synthesis routes* of these polymers are described in the Supplemental Information. It is seen that one spacer unit contains a single phenyl ring, dubbed here Pt-1; whereas the other spacer unit contains three phenyl rings, dubbed Pt-3. The NLO spectroscopies used in this work include broad-band ultrafast as well as cw pump-probe photomodulation (PM), electroabsorption (EA), and two-photon absorption (TPA). We complete our investigation by comparing the NLO spectra with linear optical measurements such as absorption and photoluminescence (PL) spectra. We note that absorption and TPA spectroscopy probe electronic excited states with *odd* or *even* symmetry, respectively; and consequently are complementary to each other. Whereas EA spectroscopy is sensitive to excited states of both *odd* and *even* symmetry. These extensive experimental techniques and quantum-chemical computational results reveal fascinating ultrafast dynamics of the ISC owing to the excited state order and enhanced SOC that is controlled by the chemical composition and structure of these Pt-polymers.

Results

(i) Linear and nonlinear optical spectroscopies. The PL spectra of Pt-1 and Pt-3 films (Fig. 1(b)) show both fluorescence (FL; 2.6–3.2 eV) and phosphorescence (PH; 1.5–2.5 eV) emission bands. The FL (PH) band is assigned to transitions from the lowest singlet (triplet) excited state, S_1 (T_1) into the ground state, S_0 (or $1A_g$)¹². The PH 0–0 line is much narrower than the 0–0 FL band and has been recently interpreted as due to super-radiance emission¹³. The intense vibronic side-bands observed in the triplet emission spectrum result from the large displacement between the S_0 and T_1 optimal geometries¹⁴. The S_1 - T_1 energy difference, ΔE is estimated to be 0.7 eV and 0.8 eV for the Pt-1 and Pt-3, respectively; in agreement with other π -conjugated polymers¹⁵. The most distinct difference between Pt-1 and Pt-3 emission spectra is the relatively weak FL emission in Pt-1; this indicates that a faster ISC in this polymer reduces the FL emission intensity relative to that of the PH emission band.

In contrast to the PL spectra, the absorption spectra of Pt-1 and Pt-3 films (Figs. 1(c,d)) and solution (Figs. 2(a,b)) have multiple broad overlapping peaks that indicate contributions of many optically active excited states. Consequently, in order to elucidate the nature

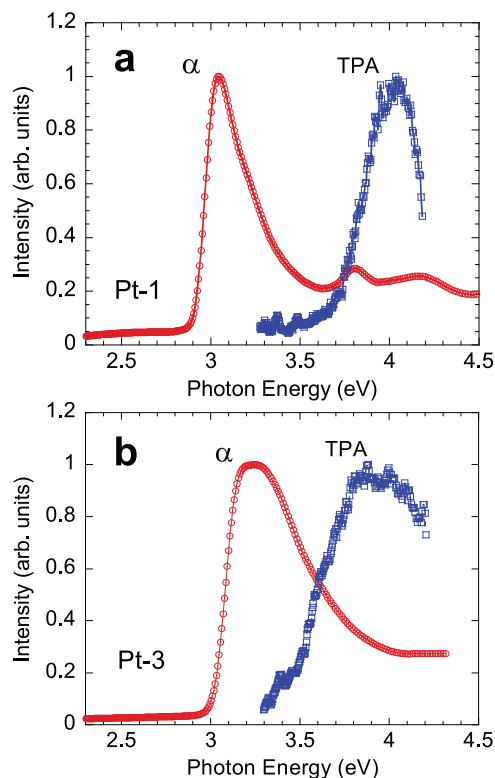


Figure 2 | Two photon absorption (TPA) spectra of Pt-1 (a) and Pt-3 (b) solutions, compared to their respective absorption spectrum (α).



of the excited states responsible for the various absorption bands, we studied the EA and TPA spectra of the two Pt-polymers (see Methods). Quantitatively EA is a third-order NLO effect, and thus may be described by the imaginary part of the third order optical susceptibility. The EA spectroscopy, where the sample is exposed to a modulated dc electric field, F , has been a sensitive tool for studying the band structure of inorganic-semiconductors¹⁶ and organic-semiconductors¹⁷ that allows for separation of absorption peaks due to tightly bound one-dimensional excitons from that of the continuum band. We note that the EA of confined exciton scales with F^2 , and its spectrum is proportional to the first derivative of the absorption with respect to the photon energy; whereas the EA related to the continuum band scales with $F^{1/3}$, and its spectrum contains Franz-Keldysh (FK) type oscillation¹⁸. In contrast, the TPA spectroscopy has been a powerful tool to study the optically forbidden A_g states in π -conjugated polymers¹⁹.

Figures 1(c,d) show the EA spectra of Pt-1 and Pt-3 films at 80 K up to 4.5 eV. Following Mazumdar *et al.* model¹⁷, four essential states ($1A_g$, $1B_u$, mA_g , and nB_u) contribute substantially to the EA spectrum of π -conjugated polymers. At low energy there is a ‘first-derivative’ like feature with zero crossing at ~ 3.17 eV (Pt-1) and ~ 3.05 eV (Pt-3) that we thus assign to the $1B_u$ exciton, accompanied by several phonon sidebands²⁰. In addition there is a prominent field-induced absorption band at higher energies at 3.9 eV (Pt-1) and ~ 3.8 eV (Pt-3) that we assign as due to the $1A_g \rightarrow mA_g$ transition, which becomes partially allowed by the symmetry breaking induced by the electrical field. These mA_g states appear as inhomogeneous broadened band in the TPA spectra at ~ 4.03 eV (Pt-1) and 3.9 eV (Pt-3) (Figs. 2(a,b)). In Pt-1 (Fig. 1(c)), we see a ‘second derivative’-like feature with zero crossing at 4.15 eV attributed to the nB_u state, which is consistent with a weak linear absorption band at 4.2 eV. The EA spectrum of Pt-3 (Fig. 1(d)) at similar photon energies shows a modulation spectral feature with two zero crossings at 4.1 eV and 4.35 eV, respectively, which we ascribed to mA_g and nB_u that mix under the influence of the electric field²¹.

Importantly, compared to the absorption spectrum, the $1B_u$ EA spectral feature is very different in Pt-1 and Pt-3. The EA feature related to $1B_u$ in Pt-1 actually lies *above the absorption peak* at ~ 3.05 eV. We thus infer that the absorption onset in Pt-1 is due to a band different than the π - π^* transition, and speculate that it originates from the lowest lying $MLCT$ singlet state (as confirmed by quantum chemistry calculations, see below); whereas the EA derivative feature points to the lowest π - π^* electronic character singlet state ($1B_u$) at ~ 3.17 eV. A splitting of ~ 0.12 eV between the lowest lying $MLCT$ state and that of the π - π^* state is in good agreement with the theory (see below). The lack of EA intensity for $MLCT$ state could be due to its localization nature, for which the external field is too small of a perturbation to cause sizable changes in its related optical transitions. The diminished EA feature from the $MLCT$ state that lies below $1B_u$ in Pt-1 indicates weak coupling between the $MLCT$ and mA_g of the π - π^* manifold.

To further elucidate the excited state properties of Pt-1, we synthesized a π -conjugated polymer similar to Pt-1 but without the Pt-containing group. Compared to Pt-1, the absorption onset of a deposited film of this non-Pt polymer is at ~ 3.2 eV (see broken line in Fig. 1(c)), which is at the energy level of the $1B_u$ exciton in Pt-1 deduced from the EA spectrum. This is additional evidence that the absorption onset of Pt-1 originates from the lowest lying $MLCT$ singlet state rather than from the π - π^* transition.

We also note that the absorption spectra in solution (Fig. 2(a)) and film (Fig. 1(c)) are very similar for the Pt-1 polymer. This shows that the lowest singlet state in Pt-1 is quite robust, in agreement with a localized $MLCT$ state. In contrast, $E(1B_u)$ in Pt-3 solution (Fig. 2(b)) is blue-shifted by ~ 0.1 eV as compared to the film (Fig. 1(d)), because in this polymer the lowest singlet exciton has π - π^* electron character. This indicates that the states related with $MLCT$ do not

show the usual solid state effect, probably due to their more localized character. Moreover compared to the robust energy of $MLCT$ states, the obtained change in $E(mA_g)$ between film (Fig. 1(c,d)) and solution (Fig. 2(a,b)) in both Pt-polymers gives another evidence that the π -electron singlet states are more spatially extended than the $MLCT$.

Overall, no FK type oscillation related to the onset of the interband transition is seen in the EA spectra of both polymers. We thus conclude that the π -electron states in Pt polymers are better described in terms of *excitons*. Assuming the continuum band in π -conjugated polymers to be very close to $E(nB_u)$ ²², we may estimate the intrachain exciton binding energy, E_b in the two polymers as $E_b = E(nB_u) - E(1B_u)$. This yields $E_b \approx 1$ eV for Pt-1 and $E_b \approx 1.1$ eV for Pt-3. This large intrachain E_b is in agreement with other measured E_b values in the class of π -conjugated polymers²³. However, for Pt-1 the lowest excited state is $MLCT$ and therefore E_b estimate in this case is not as clear.

(ii) Theoretical calculations. Our theoretical modeling confirms the conclusions that the excited state structure in Pt-1 and Pt-3 polymers is indeed different as obtained in the experiment discussed above. Figure 3 shows schematic ordering of the singlet and triplet manifolds of Pt-1 and Pt-3 that emerge from our work. In addition, the obtained Natural Transition Orbitals (NTOs) of the relevant low-energy excited states are displayed in Fig. 4. We found that the strongly allowed optical transition $1A_g \rightarrow 1B_u$ (S_n) in Pt-1 is a π - π^* transition that is characteristic for π -conjugated polymers^{24,25}, where both electron and hole are delocalized over the conjugated backbone with only a small participation of Pt atoms (Fig. 4(a)). However, the lowest state in Pt-1 (S_1) is $MLCT$ with significant charge-transfer character as schematically shown in Fig. 3(a). Indeed, the calculated NTOs (Fig. 4(b)) show that in this excited state the electron becomes strongly localized on the Pt atom,

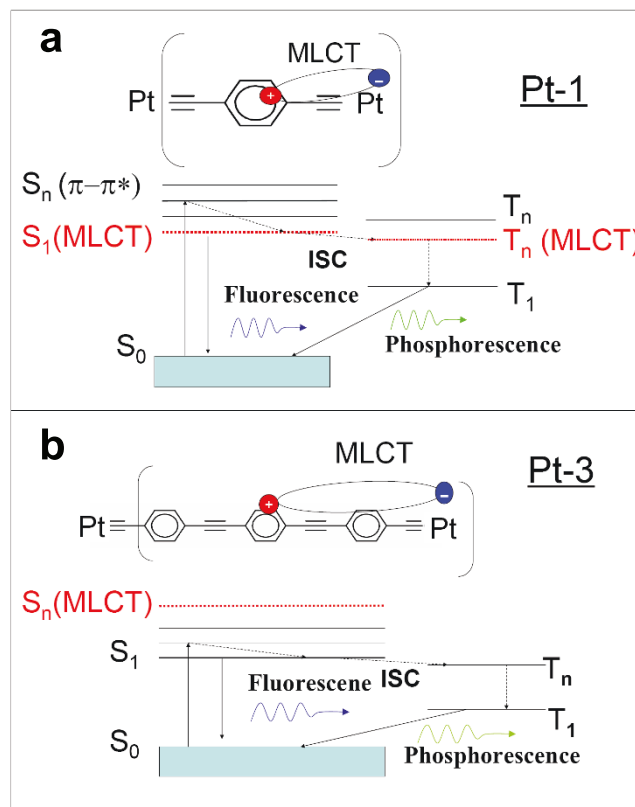


Figure 3 | Illustration of Metal-to-Ligand Charge Transfer ($MLCT$) state with electron in the platinum atom orbital and hole in the π -conjugated spacer. Also schematically depicted are the energy levels of the singlet and triplet manifolds of Pt-1 (a) and Pt-3 (b). ISC: intersystem crossing.

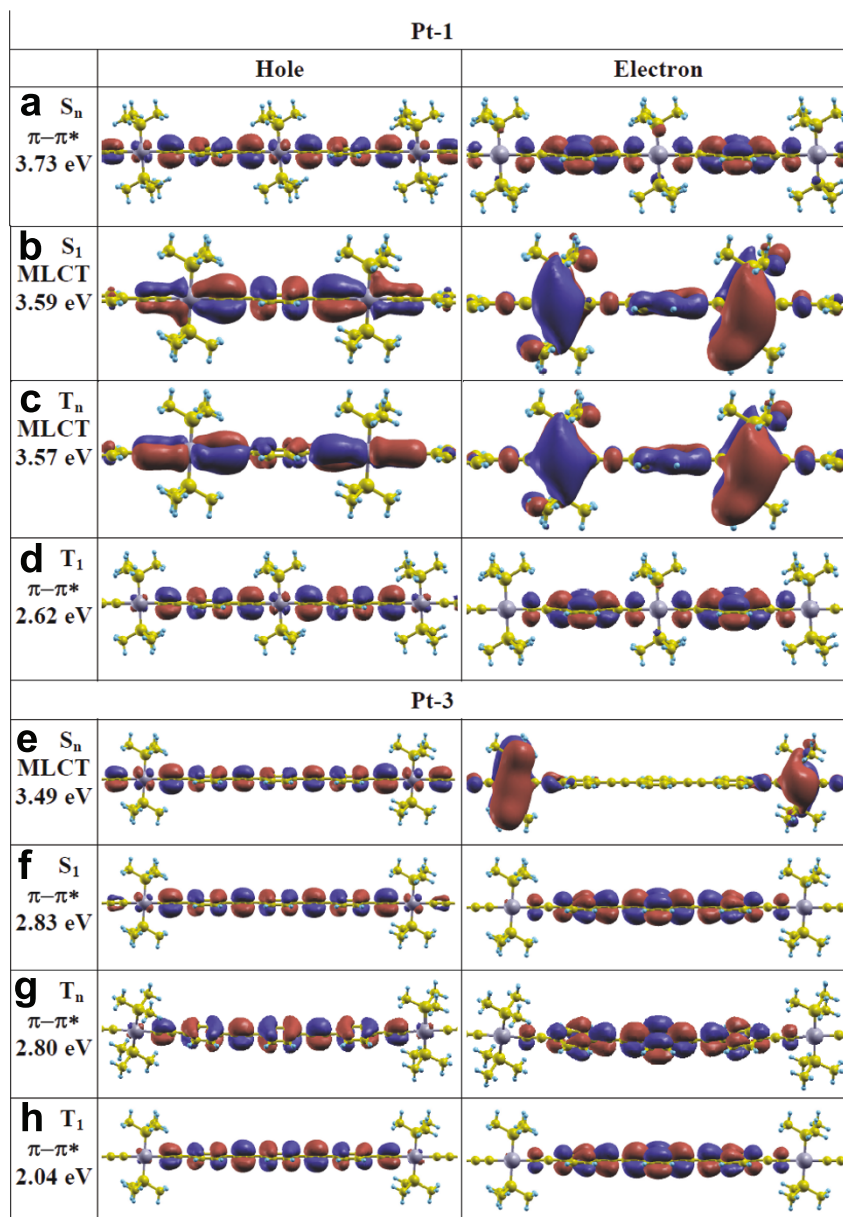


Figure 4 | Calculated natural transition orbitals that characterize the essential lowest electronic states which define the photoexcitation dynamics in Pt-1 and Pt-3 polymers.

whereas the hole remains delocalized over the conjugated backbone. We note that the absolute values of the calculated excitation energies are systematically blue shifted compared to the experimental data, since they are strongly dependent on the hybrid DFT model used in calculations (see Methods); however the relative trends are well reproduced. For example, the splitting between $E(1B_u)$ and the lowest $E(MLCT)$ in Pt-1 is calculated to be 0.14 eV, close to the experimental value of 0.12 eV. The situation is opposite in Pt-3 system, where $E(MLCT)$ S_n (Fig. 4(e)) is *higher* than $E(1B_u)$ $\pi-\pi^*$ (S_1) (Fig. 4(f)). The lowering of $\pi-\pi^*$ transition energy in Pt-3 is attributed to the larger conjugation segment length between the Pt-atoms (the latter partially break the π -conjugation, see $\pi-\pi^*$ orbitals in Fig. 4). However, $E(MLCT)$ does not change substantially when going from Pt-1 to Pt-3 polymers. While $E(MLCT)$ may red-shift as a result of better conjugation, this effect is partially cancelled due to smaller electron-hole binding energy in Pt-3 $MLCT$ caused by the larger effective separation between charges, as compared to Pt-1.

Our calculations also suggest a more efficient ISC process in Pt-1 compared to that in Pt-3, which is confirmed by the experimental

data (discussed below). Namely, the fast internal conversion within the singlet manifold in Pt-1 populates the lowest singlet $MLCT$ state. The corresponding triplet $MLCT$ state (T_n in Fig. 3(a) and Fig. 4(c)) has the same nature and a very similar energy to the S_1 $MLCT$ state. Localization of the electron on the Pt atom leads to an efficient ISC (where the electron spin is flipped) due to the enhanced SOC. Subsequently, the internal conversion process within the triplet manifold populates the lowest triplet state, T_1 (Fig. 3(a)), which has $\pi-\pi^*$ character (Fig. 4(d)) from where the phosphorescence emission originates. In contrast, the ISC process in Pt-3 occurs between S_1 (Fig. 4(f)) and T_n (Fig. 4(g)) states both having $\pi-\pi^*$ character (Fig. 3(b)), since the lowest $MLCT$ state lies higher than the lowest $\pi-\pi^*$ state in this system. Consequently, the ISC process in Pt-3 is less favorable process, since $\pi-\pi^*$ transitions have smaller effective SOC constant.

(iii) Transient and steady state photomodulation spectroscopy. For studying the ISC dynamics in the two Pt-polymers, we explored the ultrafast photoexcitation kinetics using the time-resolved



photomodulation (PM) technique. Figure 5(a) shows the transient PM spectrum of Pt-1 solution at various delay times, t , following the pump pulse excitation. The PM spectrum contains three PA bands: PA₁ at ~ 0.75 eV, PA₂ at ~ 2.5 eV, and a broad PA band (TA) at ~ 1.9 eV, which partially overlaps with PA₂. The bands PA₁ and PA₂ (fast components) are correlated since they decay together with a time constant, $\tau < \sim 1$ ps. The band PA₁ (~ 0.75 eV) in fact coincides with the energy difference $E(mA_g) - E(1B_u)$ extracted from the EA and TPA spectra above, and thus is assigned as $1B_u \rightarrow mA_g$ optical transition that originates from the photogenerated singlet excitons. The energy difference $E(MLCT) - E(mA_g)$ (~ 0.95 eV) indicates that PA₁ cannot be due to the transition $MLCT \rightarrow mA_g$; this conclusion is also consistent with the lack of EA signal from the $MLCT$ states, as discussed above. The band PA₂ is interpreted as due to the transition $1B_u \rightarrow kA_g$ from the same singlet excitons, in analogy with other π -conjugated polymers²⁶. We thus conclude that the primary excitations in Pt-1 are still π - π^* excitons, even that the $MLCT$ state is the lowest singlet exciton in this polymer. This happens since the pump pulse predominantly populates the π - π^* manifold, and there is little interaction between the π - π^* and $MLCT$ states during the ultrafast hot exciton thermalization process.

Figure 5(b) shows the steady state PM spectrum of Pt-1 films. The spectrum is dominated by a broad PA band that peaks at ~ 1.95 eV, which we interpret as due to triplet-triplet transition from the lowest π - π^* triplet, T_1 , since it has the same dynamics as that of the PH emission band in this polymer¹³. This cw PA band is very similar to the broad TA band obtained in the ps time domain; and we thus interpret the ultrafast TA band as due to triplet excitons. Consequently, the ultrafast decay of bands PA₁ and PA₂ into the TA band is caused by the ISC process from the singlet to the triplet π - π^* manifolds. We thus conclude that the ISC process in Pt-1 is much faster than in any other π -conjugated polymer (apart from triplet formation via singlet fission). The reason for the ultrafast ISC in this Pt-polymer is the much stronger SOC that is due to the ‘heavy atom effect’ of the intrachain Pt atoms. A more rigorous comparison between a Pt-polymer and its non-Pt analog (that have a different structure than Pt-1) is shown in the Supplement Information (Fig. S-2). It shows again that the PA bands related to the π - π^* singlet exciton decay much faster in the Pt-polymer compared to the non-Pt polymer analog.

Figure 5 (c, d) shows the transient PM spectrum of Pt-3 solution at various times, t . As in Pt-1 the spectrum here also contains three PA bands: PA₁ at ~ 0.7 eV, PA₂ at 1.7 eV and a relatively broad TA band at 1.8 eV that overlaps with PA₂. The bands PA₁ and PA₂ are correlated since they decay together with $\tau \sim 6$ ps. Similar as in Pt-1 we interpret the ultrafast PA bands in Pt-3 as due to singlet excitons in the π - π^* manifold, and thus their decay reflects the ISC process dynamics in this polymer. The substantially slower obtained ISC process in Pt-3 explains the relative stronger cw FL emission of this polymer compared to that of Pt-1 (Fig. 1). The dominant PA band (T) in the cw PM spectrum at 1.7 eV is interpreted as due to $T_1 - T_n$ transitions in the triplet manifold, and thus the PA band in Fig. 5(a) reflects the transient triplet PA. We note, however, that the cw PM spectrum of Pt-3 may have some contribution from polarons since a PA band related to polarons is observed below ~ 0.5 eV²⁷.

Discussion

In this work two Pt-containing polymers (namely Pt-1 and Pt-3) with different organic spacer length in between each two adjacent intrachain Pt atoms were synthesized and extensively studied using a variety of NLO spectroscopies that include electroabsorption, two-photon absorption, and ultrafast and steady state photomodulation. The NLO spectra were compared to the absorption and luminescence spectra. From quantum chemistry calculation and the NLO measurements we conclude that the lowest singlet state in Pt-1 is a Metal-to-Ligand Charge Transfer ($MLCT$) state, which lies below the lowest π - π^* exciton; however, the order is reversed in Pt-3. Surprisingly, the primary photoexcitations in both polymers are singlet π - π^* excitons, irrespective of the excited state order. We note, however that the electron in the $MLCT$ state is localized on the Pt atom center orbital. Consequently the $MLCT$ states have relatively large SOC and their energy is practically independent on the linker length. In contrast the energy of the π - π^* transitions substantially depend on the linker length. Because of the π -electron delocalization within the π -conjugated linker, the π - π^* $1B_u$ state has relatively weak SOC, which is further reduced for longer linker. This rationalizes our experimental results of the way the intrachain Pt atom influences the ISC rate in both Pt-1 and Pt-3.

From the ps transient decay of the photogenerated π - π^* excitons we deduce a record ISC timescale of $< \sim 1$ ps and ~ 6 ps in Pt-1 and

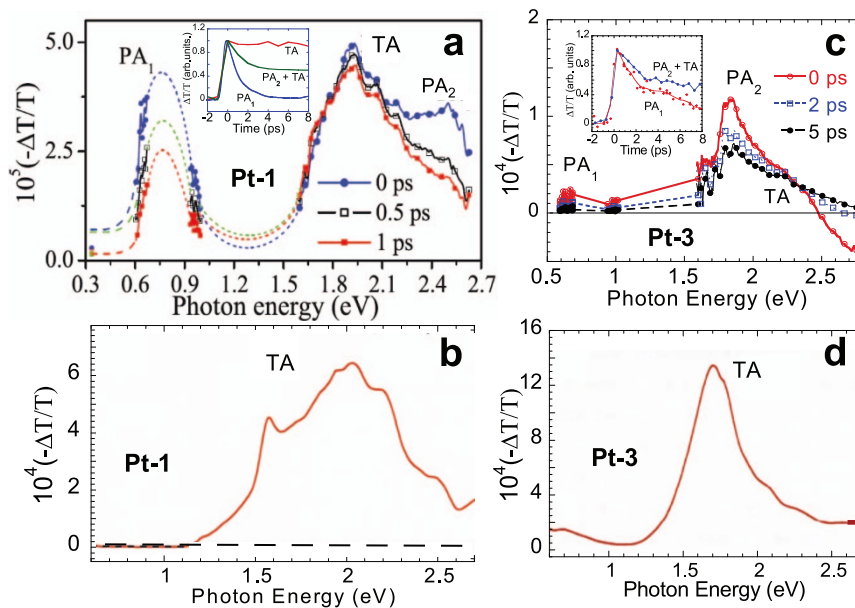


Figure 5 | (a), Transient photomodulation (PM) spectrum of Pt-1 solution at various time, t following the pump pulse excitation. The PA bands PA₁, PA₂, and TA are assigned. The inset in (a) shows the transient decay dynamics of the main PA bands assigned in (a). (b), The steady state PM spectrum of Pt-1 film measured at 40 K; The TA band is assigned. (c) and (d), same as (a) and (b), but for Pt-3.



Pt-3, respectively. The larger ISC rate in Pt-1 is attributed to stronger SOC that originates from the localized *MLCT* singlet and triplet states through which the ISC transition may occur. Such energetics is attributed to a smaller spacer between adjacent intrachain Pt atoms. We conclude that the controllable spacer between the intrachain Pt atoms not only tunes the effective spin-orbit coupling, but also influences the excited state order of the *MLCT* and π - π^* states. This implies synthetic design strategies to achieve optimal photoexcitation spin dynamics in metal-containing π -conjugated polymers for organic OLED and OPV technologies. In particular, Pt-polymers with larger spacer in between each adjacent Pt-atoms may have smaller ISC rate and consequently larger fluorescence emission, which may be readily used for white OLEDs.

Methods

CW spectroscopies. The absorption spectrum was measured with a Cary UV-Vis-NIR spectrometer. For the cw PL emission, an Ar⁺ laser beam at 3.5 eV was used to excite the Pt-polymer films that were kept at 40 K under dynamic vacuum. The PL emission was collected using a large F-number lens, and spectrally and spatially filtered to eliminate the excitation laser light. Corrections due to the system spectral response and wavelength to photon energy transformation were readily done. The steady state PM spectrum was obtained using a standard setup²⁸ with pump excitation from an Ar⁺ laser beam at $\hbar\omega = 3.5$ eV. The pump beam was modulated at frequency, $f = 300$ Hz by a mechanical chopper. A beam from an incandescent tungsten/halogen lamp was used as the probe. The PM spectrum in the form of $(-\Delta T/T)$, where ΔT is the change in the transmission, T induced by the pump was measured using a lock-in amplifier referenced at f . For obtaining the PM spectrum in the broad spectral range of $0.4 < \hbar\omega(\text{probe}) < 2.7$ eV, we used a monochromator and various combinations of gratings, filters, and solid-state photodetectors such as Si, Ge, and InSb, each combined with suitable preamplifier.

Transient spectroscopies. For the transient PM spectroscopy we used the fs two-color pump-probe correlation technique with two laser systems based on Ti:Sapphire oscillator^{20,29}: a low power (energy/pulse ~ 0.1 nJ) high repetition rate (~ 80 MHz) laser for the mid-ir spectral range; and a high power (energy/pulse ~ 10 μ J) low repetition rate (~ 1 kHz) laser for the near-IR/visible spectral range. In both laser systems the pump excitation was set at $\hbar\omega = 3.1$ eV. For the low intensity measurements we used an optical parametric oscillator (Opal, Spectral-Physics) that generates probe $\hbar\omega$ continuously changing from 0.55 to 1.05 eV, and from 0.14 to 0.43 eV, respectively²⁹. For the high intensity measurements, white light supercontinuum was generated for the probe $\hbar\omega$ ranging from 1.15 to 2.7 eV. In general, the transient PM signal, $\Delta T/T(t)$ is negative for photoinduced absorption (PA) and positive for photo-bleaching (PB)²⁰. The transient PM spectra from the two laser systems were normalized to each other in the near-IR/visible spectral range, for which the IR probe photon energy from the low power laser system was doubled.

TPA measurements. The TPA spectrum was measured using the polarized pump-probe correlation technique with the low repetition rate high-power laser system at time delay $t = 0^{\text{th}}$. The linearly polarized pump beam was set at 1.55 eV, which is much below the polymer absorption band; whereas the probe beam from the white light super-continuum covered the spectral range from 1.7 to 2.8 eV. The temporal and spatial overlap between the pump and probe beams on the sample film leads to PA signal that peaks at $t = 0$; this transient PA has a temporal profile identical to the cross-correlation trace of the pump and probe pulses³⁰. The ultrafast PA is TPA of one pump photon and one probe photon, of which spectrum yields the TPA spectrum in the spectral range between 3.25 to 4.35 eV.

EA spectroscopy. For the EA measurements we used thin polymer films spin cast on an EA substrate template^{20,23}. The EA template consisted of two interdigitated sets of a few hundred 30 μ m wide gold electrodes, which were patterned on a sapphire substrate. The sample was placed in a cryostat for low temperature measurements. We applied an oscillatory potential, V to the electrodes, with $V = 300$ Volts and $f = 1$ kHz; with these parameters a typical electric field, $F \sim 10^5$ Volt/cm parallel to the film was generated. For obtaining the EA spectrum we used an incandescent light source from a Xe lamp, which was dispersed through a monochromator before impinging on the sample, and detected by a UV-enhanced silicon photodiode. We measured ΔT using a lock-in amplifier set to twice the frequency ($2f$) of the applied field²³, and verified that no EA signal was observed at f or $3f$. ΔT and T spectra were measured separately, and the EA spectrum was obtained from the ratio $\Delta T/T$.

Computational methodology. We calculated singlet and triplet states of Pt-1 and Pt-3 oligomers of various oligomer length (up to 10–15 nm) in order to extrapolate to the polymer limit. In our model we terminate the polymer backbone by an H-atom after the first phenyl ring adjacent to the Pt-atom, and replace the *n*-Bu side-chain groups attached to Pt with CH₃ to speed up the quantum-chemical calculations. Specifically, the computational results presented here are for Pt-1 (Pt-3) oligomer comprised of 5 (3) repeat units (i.e., containing 5 (3) embedded platinum atoms). The ground state geometries were optimized using Density Functional (DFT) methodology, and the

excited states were calculated using time-dependent DFT (TDDFT) technique. These are currently methods of choice for quantum-chemical modeling of ground and excited state electronic properties in molecules of intermediate size. For all simulations we used hybrid B3LYP³¹ functional coupled with LANL2dz* (Pt)/6-31G* (all other atoms) basis set as implemented in the Gaussian09 suite³². Such model chemistry has shown an excellent quantitative performance in similar organometallic compounds in a number of previous studies^{33,34}. 20 lowest singlet (triplet) states have been calculated and analyzed using the natural transition orbital (NTO) approach³² to determine their characteristic nature. A moderately polar solvent, ethanol ($\epsilon = 24.9$), is included in this study via the conductor-like polarizable continuum model (CPCM) as implemented in Gaussian09 software package³² in order to mimic the polymer's polarizable dielectric environment. Even though this may be an overestimation of the dielectric constant, the effects of this dielectric medium throughout our study are minor and the conclusions are the same as for the simulations in the gas phase.

- Zhen, C. G. *et al.* Achieving Highly Efficient Fluorescent Blue Organic Light-Emitting Diodes Through Optimizing Molecular Structures and Device Configuration. *Adv. Func. Mater.* **21**, 699–707 (2011).
- Sun, Y. R. *et al.* Management of singlet and triplet excitons for efficient white organic light-emitting devices. *Nature* **440**, 908–912 (2006).
- Schlenker, C. W. *et al.* Polymer triplet energy levels need not limit photocurrent collection in organic solar cells. *J. Am. Chem. Soc.* **134**, 19661–19668 (2012).
- Dyer-Smith, C. *et al.* Triplet Formation in Fullerene Multi-Adduct Blends for Organic Solar Cells and Its Influence on Device Performance. *Adv. Func. Mater.* **20**, 2701–2708 (2010).
- Ho, C.-L. & Wong, W.-Y. Metal-containing Polymers: Facile Tuning of Photophysical Traits and Emerging Applications in Organic Electronics and Photonics. *Coord. Chem. Rev.* **255**, 2469–2502 (2011).
- Hoffmann, S. T. *et al.* Spectral diffusion in poly(para-phenylene)-type polymers with different energetic disorder. *Phys. Rev. B* **81**, 115103 (2010).
- Furuta, P. T., Deng, L., Garon, S., Thompson, M. E. & Frechet, J. M. J. Platinum-Functionalized Random Copolymers for Use in Solution-Processible, Efficient, Near-White Organic Light-Emitting Diodes. *J. Am. Chem. Soc.* **126**, 15388–15389 (2004).
- Wilson, J. S. *et al.* Spin-dependent exciton formation in π -conjugated compounds. *Nature* **413**, 828–831 (2001).
- Köhler, A. & Bäessler, H. What controls triplet exciton transfer in organic semiconductors? *J. Mater. Chem.* **21**, 4003–4011 (2011).
- O'Keefe, G. E. *et al.* Femtosecond transient photoinduced transmission measurements on a novel conjugated zinc porphyrin system. *J. Chem. Phys.* **104**, 805–812 (1996).
- Wang, X., Goeb, S., Ji, Z. & Castellano, F. N. The Excited State Absorption Properties of Pt(II) Terpyridyl Complexes Bearing π -Conjugated Arylacetylide. *J. Phys. Chem. B* **114**, 14440–14449 (2010).
- Wilson, J. S. *et al.* Triplet states in a series of Pt-containing ethynylenes. *J. Chem. Phys.* **113**, 7627–7635 (2000).
- Khachatryan, B., Nguyen, T. D., Vardeny, Z. V. & Ehrenfreund, E. Phosphorescence superradiance in a Pt-containing π -conjugated polymer. *Phys. Rev. B* **86**, 195203 (2012).
- Beljonne, D. *et al.* Spatial extent of the singlet and triplet excitons in transition metal-containing polyynes. *J. Chem. Phys.* **105**, 3868–3877 (1996).
- Köhler, A. & Beljonne, D. The Singlet-Triplet Exchange Energy in Conjugated Polymers. *Adv. Func. Mater.* **14**, 11–18 (2004).
- Willardson, R. K. & Beer, A. C. *Semiconductors and Semimetals*, Vol. **9**, (Academic Press, New York, 1972).
- Guo, D. *et al.* Role of the conduction band in electroabsorption, two-photon absorption, and third-harmonic generation in polydiacetylenes. *Phys. Rev. B* **48**, 1433–1459 (1993).
- Sebastian, L. & G. Weiser, G. One-Dimensional Wide Energy Bands in a Polydiacetylene Revealed by Electroreflectance. *Phys. Rev. Lett.* **46**, 1156–1159 (1981).
- Chandross, M. *et al.* Optical absorption in the substituted phenylene-based conjugated polymers: Theory and experiment. *Phys. Rev. B* **55**, 1486–1496 (1997).
- Tong, M., Sheng, C.-X. & Vardeny, Z. V. Nonlinear optical spectroscopy of excited states in polyfluorene. *Phys. Rev. B* **75**, 125207 (2007).
- Sheng, C.-X., Tong, M. & Vardeny, Z. V. Nonlinear optical spectroscopy of excited states in disubstituted polyacetylene. *Phys. Rev. B* **81**, 205103 (2010).
- Martin, R. L. Natural transition orbitals. *J. Chem. Phys.* **118**, 4775–4777 (2003).
- Liess, M. *et al.* Electroabsorption spectroscopy of luminescent and nonluminescent π -conjugated polymers. *Phys. Rev. B* **56**, 15712–15724 (1997).
- Nayyar, I. *et al.* Localization of Electronic Excitations in Conjugated Polymers Studied by DFT. *J. Phys. Chem. Lett.* **2**, 566–571 (2011).
- Magyar, R. J., Tretiak, S., Gao, Y., Wang, H.-L. & Shreve, A. P. A joint theoretical and experimental study of phenylene-acetylene molecular wires. *Chem. Phys. Lett.* **401**, 149–156 (2005).
- Zhao, H., Mazumdar, S., Sheng, C.-X., Tong, M. & Vardeny, Z. V. Photophysics of excitons in quasi-one-dimensional organic semiconductors: Single-walled carbon nanotubes and π -conjugated polymers. *Phys. Rev. B* **73**, 075403 (2006); and references therein.



27. Yang, C. *et al.* Spectroscopic study of spin-dependent exciton formation rates in π -conjugated semiconductors: Comparison with electroluminescence techniques. *Phys. Rev. B* **70**, 241202(R) (2004).
28. Jiang, X. M. *et al.* Spectroscopic Studies of Photoexcitations in Regioregular and Regiorandom Polythiophene Films. *Adv. Funct. Mater.* **12**, 587–597 (2002).
29. Sheng, C.-X., Tong, M., Singh, S. & Vardeny, Z. V. Experimental determination of the charge/neutral branching ratio η in the photoexcitation of π -conjugated polymers by broadband ultrafast spectroscopy. *Phys. Rev. B* **75**, 085206 (2007).
30. Singh, S. *Ultrafast photophysics of π -conjugated polymers and polythiophene/fullerene blends for organic photovoltaic applications*, Ph. D. thesis, University of Utah, 2010.
31. Becke, A. D. A new mixing of Hartree–Fock and local density-functional theories. *J. Chem. Phys.* **98**, 1372 (1993).
32. Frisch, M. J. *et al.* Gaussian-09, Revision A.1, Gaussian Inc., Wallingford CT, 2009.
33. Campbell, I. H. *et al.* Excitation transfer processes in a phosphor-doped poly(p-phenylene vinylene) light-emitting diode. *Phys. Rev. B* **65**, 085210 (2002).
34. Kuposov, A. Y. *et al.* Formation of assemblies comprising Ru-polypyridine complexes and CdSe nanocrystals studied by ATR-FTIR spectroscopy and DFT modeling. *Langmuir* **27**, 8377–83 (2011).

Acknowledgments

We thank L. Wojcik for the synthesis of the two Pt-containing polymers, as well as the non-Pt polymer. We also thank T. Nguyen for helpful discussion, J. Holt for help with the ps measurements, and Y. Zhai for the non-Pt absorption spectrum. The work at the University of Utah was supported by the DOE grant No. DE-FG02-04ER46109 (the Pt and non-Pt synthesis, transient and cw PM and TPA measurements), and the NSF-MRSEC, grant

DMR-1121252 (the EA measurements). C.-X.S. acknowledges the support of NSFC grant No. 61006014, 863 Program of China No. 2011AA050520, and the Fundamental Research Funds for the Central Universities No. 30920130111008. S.T. acknowledges the support from the US Department of Energy and Los Alamos National Laboratory (LANL) Directed Research and Development Funds.

Author contributions

M.T. and A.G. were responsible for the transient PM measurements in the visible and mid-IR, respectively; S.S. was responsible for the EA and TPA measurements; T.D. was responsible for the cw spectroscopies; A.G. and C.-X.S. were responsible for the experimental figures; C.-X.S. also wrote the first draft of the manuscript; S.T. was responsible for the quantum chemical calculations and manuscript second draft; Z.V.V. was responsible for the project planning, group managing, and final writing.

Additional information

Supplementary information accompanies this paper at <http://www.nature.com/scientificreports>

Competing financial interests: The authors declare no competing financial interests.

How to cite this article: Sheng, C.-X. *et al.* Ultrafast intersystem-crossing in platinum containing π -conjugated polymers with tunable spin-orbit coupling. *Sci. Rep.* **3**, 2653; DOI:10.1038/srep02653 (2013).



This work is licensed under a Creative Commons Attribution-NonCommercial-ShareAlike 3.0 Unported license. To view a copy of this license, visit <http://creativecommons.org/licenses/by-nc-sa/3.0>